Vol 16 No 3, March 2007
1009-1963/2007/16(03)/0650-10
Chinese Physics
© 2007 Chin. Phys. Soc.
and IOP Publishing Ltd

Atomic population oscillations between two coupled Bose–Einstein condensates with time-dependent nonlinear interaction*

Li Fei(李 飞)†, Shu Wei-Xing(舒维星), Luo Hai-Lu(罗海陆), and Ren Zhong-Zhou(任中洲)

Department of Physics, Nanjing University, Nanjing 210093, *China*

(Received 2 June 2006; revised manuscript received 20 September 2006)

The atomic population oscillations between two Bose–Einstein condensates with time-dependent nonlinear interaction in a double-well potential are studied. We first analyse the stabilities of the system's steady-state solutions. And then in the perturbative regime, the Melnikov chaotic oscillation of atomic population imbalance is investigated and the Melnikov chaotic criterion is obtained. When the system is out of the perturbative regime, numerical calculations reveal that regulating the nonlinear parameter can lead the system to step into chaos via period doubling bifurcations. It is also numerically found that adjusting the nonlinear parameter and asymmetric trap potential can result in the running-phase macroscopic quantum self-trapping (MQST). In the presence of a weak asymmetric trap potential, there exists the parametric resonance in the system.

Keywords: Bose–Einstein condensates, Melnikov chaotic criterion, period doubling, macroscopic quantum self-trapping
PACC: 0530, 0545

1. Introduction

The observations of Bose–Einstein condensates (BECs)[1−3] in various dilute trapped alkali-metal atom gases have aroused the intense interest in the properties of Bose–Einstein condensates. Much research work has been done theoretically and experimentally to explore and understand this newly observed state of matter. In recent years considerable attention has been paid to the systems of two coupled Bose–Einstein condensates in a double-well trap.[4−22] The coherent atomic tunnelling between the two wells has been extensively studied.[9−22] It is found that the atomic tunnelling results from macroscopic quantum coherence of the two BECs[11, 14] and can systematically be manipulated by an appropriate time-dependent variation of the double-well potential.[18] When the double well potential is a periodical function of time, chaotic tunnelling can appear between the two condensates.[13,15−17,21] The Melnikov function approach has been used to obtain the conditions for the existence of chaotic macroscopic quantum-tunnelling.[15,16] Recently, a detailed numerical study of two coupled time-dependent Gross–Pitaevskii equation for BEC in three spatial dimensions has been presented and the effect of periodically varying the trap frequency has been numerically investigated.[19] Because of it's similarity to a two-level model, the two-coupled BEC system is also used to study nonlinear evolution of quantum states.[22]

In these theoretical researches, one of the most interesting findings is the macroscopic quantum self-trapping (MQST),[11−16,18] where the atoms show asymmetric distribution as if most atoms are trapped in one well, namely, the time-averaged population imbalance is a nonzero value. Recently, Albiez *et al*[20] reported the first experimental observation of macroscopic quantum self-trapping, which inhibits large amplitude tunnelling oscillations. After quantitative analysis of their experimental results Albiez *et al* also pointed out that the corresponding relative phase associated with the observed MQST increases monotonically (running phase modes[12]).

As narrated above, the influence of time-dependent trap potentials has been deeply investigated. Nowadays, advanced experimental techniques have made it possible to obtain time-dependent

*Project supported by the National Natural Science Foundation of China (Grant Nos 10125521 and 10535010) and the Key Development Program for State Basic Research of China (Grant No G2000077400).
†Correspondence author. E-mail: wiselfhhy@gmail.com

nonlinear interactions by adjusting the s-wave scattering length with magnetic-field-induced Feshbach resonances.[23−25] An important application of this technique is to effectively control the collapse in Bose–Einstein condensates.[23,25] Stable ^{85}Rb condensates with thousands of atoms, which would otherwise collapse if consisting of more than about 80 atoms, have been created.[23]

In this paper, we consider the role played by time-dependent atom–atom interaction in the atomic population oscillations between two coupled BECs. Firstly, we investigate the stabilities of the system's steady-state solutions. And then through the direct perturbation technique we obtain a general solution of the perturbed equation. We find that the boundedness condition of the general solution contains Melnikov chaotic criterion. Hai's group has paid much attention to the chaotic dynamics of BECs.[13,16,26−33] In their work the direct perturbation and Melnikov function methods are extensively used,[13,16,26−29,33] The two methods are also used to investigate the chaotic population oscillations in the present work. In the unperturbed regime, numerical calculations reveal that the nonlinear interatomic interaction has a crucial influence on the oscillations of the fractional population imbalance while stepping into chaos via period doubling bifurcations. Bifurcations have also been found in two-component BECs coupled with laser or/and radio-frequency pulses.[34] The macroscopic quantum self-trapping is numerically explored and our result is in agreement with the experimental result reported in Ref.[20]. The parametric resonance is also numerically demonstrated when the trapping potential is a weak asymmetric one.

2. The system

The macroscopic quantum wave function $\Psi(x,t)$ characterizing a weakly interacting BEC in a trapping potential $V_{\rm tr}(\boldsymbol{r})$ near-zero temperature satisfies the mean-field Gross–Pitaevskii (GP) equation

$$\mathrm{i}\hbar\frac{\partial\Psi}{\partial t} = -\frac{\hbar^2}{2m}\bigtriangledown^2\,\Psi + V_{\rm tr}\,\Psi + g|\,\Psi|^2\,\Psi, \qquad (1)$$

where $\hbar$ is Planck's constant, $g = 4\pi a_{\rm s}\hbar^2/m$ is the nonlinearity parameter that takes into account the mean field produced by the other bosons, and $a_{\rm s}$ is the s-wave scattering length of atoms that can be either positive or negative. $a_{\rm s} > 0$ indicates a repulsive interaction and $a_{\rm s} < 0$ corresponds to an attractive case. We consider the atomic population oscillations between two coupled Bose–Einstein condensates with time-dependent nonlinear interaction in a double-well potential. To this end, we select the solution of Eq.(1) in the form of two-mode approximation as follows:[11−13]

$$\Psi(\boldsymbol{r},t) = \psi_1(t)\,\Phi_1(\boldsymbol{r}) + \psi_2(t)\,\Phi_2(\boldsymbol{r}), \qquad (2)$$

with ψ_1 and ψ_2 being complex time-dependent amplitudes and Φ_1 and Φ_2 ground-state solutions in the two wells, respectively. Substituting Eq.(2) into Eq.(1) and integrating over spatial coordinates, we obtain a two-mode model for $\psi_1(t)$ and $\psi_2(t)$

$$\mathrm{i}\hbar\frac{\partial}{\partial t}\begin{pmatrix}\psi_1(t)\\ \psi_2(t)\end{pmatrix} = H(t)\begin{pmatrix}\psi_1(t)\\ \psi_2(t)\end{pmatrix}, \qquad (3)$$

where $H(t)$ is the Hamiltonian

$$H(t) = \begin{pmatrix}E_1 + \alpha_1|\psi_1|^2 & -K\\ -K & E_2 + \alpha_2|\psi_2|^2\end{pmatrix}, \qquad (4)$$

with E_1 and E_2 being zero-point energies for each condensate, α_1 and α_2 nonlinear parameters of the two modes, and K the amplitude of the tunnelling between the two condensates. These parameters can be expressed in the form of several overlap integrals of the time-independent Gross–Pitaevskii eigenfunctions as follows:[11]

$$E_i = \int \mathrm{d}\boldsymbol{r}\Big[\frac{\hbar^2}{2m}|\nabla\Phi_i|^2 + |\,\Phi_i|^2 V_{\rm tr}\Big], \qquad (5)$$

$$\alpha_i(t) = g\int \mathrm{d}\boldsymbol{r}|\,\Phi_i|^4, \qquad (6)$$

$$K = -\int \mathrm{d}\boldsymbol{r}\Big[\frac{\hbar^2}{2m}(\nabla\Phi_1\nabla\Phi_2) + \Phi_1 V_{\rm tr}\,\Phi_2\Big] \qquad (7)$$

for $i = 1, 2$.

We write the time-dependent wave functions $\psi_1(t)$ and $\psi_2(t)$ in the common form of $\psi_1(t) = \sqrt{N_1(t)}\exp[\mathrm{i}\theta_1(t)]$ and $\psi_2(t) = \sqrt{N_2(t)}\exp[\mathrm{i}\theta_2(t)]$. As is well known, $N_1(t) = |\psi_1(t)|^2$ and $N_2(t) = |\psi_2(t)|^2$ are the numbers of particles and θ_1 and θ_2 are the phases of states in the two wells, respectively. So we have the total number of particles $N = N_1 + N_2$. For convenience, we introduce two new variables $z(t) = [N_1(t) - N_2(t)]/N$ and $\phi = \theta_2(t) - \theta_1(t)$. Here $z(t)$ and ϕ are the fractional population imbalance and the relative phase. Then we can easily obtain three differential equations

$$\dot{N} = 0, \qquad (8)$$

$$\dot{z} = -2\sqrt{1-z^2}\sin\phi - \eta z, \qquad (9)$$

$$\dot{\phi} = \Delta E + \Lambda z + \frac{2z}{\sqrt{1-z^2}}\cos\phi \qquad (10)$$

with $\Delta E = [E_1 - E_2 + (\alpha_1 - \alpha_2)/2]/K$ and $\Lambda = (\alpha_1 + \alpha_2)/(2K)$. In Eq.(9) we have considered the damping force in the form of $-\eta z$. It appears for two interacting BECs with different hyperfine levels in a single harmonic trap potential.[15,35–37] In this work we consider only the damping force in this form. It is clear from Eq.(8) that the total number of particles in the two wells is conserved. In Eqs.(8)–(10) we have rescaled the time t to a dimensionless variable $Kt/\hbar$. Accordingly, all parameters and variables in the following sections are dimensionless. It is not difficult to find that when Λ is a constant and $\Delta E = \eta = 0$ there exist many groups of steady-state solutions for Eqs.(9) and (10). For simplicity, we choose $[z = 0, \phi = 0]$ and $[z = 0, \phi = \pi]$ as examples in our stability analysis. Theoretical analysis reveals that, in the phase space of (z, ϕ), $[z = 0, \phi = 0]$ is a centre if $\Lambda > -2$ and a saddle point when $\Lambda < -2$; the point $[z = 0, \phi = \pi]$ is a saddle point (centre) when $\Lambda > 2$ ($\Lambda < 2$). According to Lyapunov stability criteria,[38] all centres are Lyapunov-stable but not asymptotically-stable because the space trajectories around them are close curves that do not run to them. Here we take the case of attractive interaction for example. By assuming $\Delta E = \eta = 0$, $\Lambda = -2.5$, and selecting different initial conditions, we plot the phase portraits of z vs ϕ in Fig.1. Figure 1(a) shows that the point $[z = 0, \phi = 0]$ is a saddle point and Fig.1(b) denotes that $[z = 0, \phi = \pi]$ is a centre.

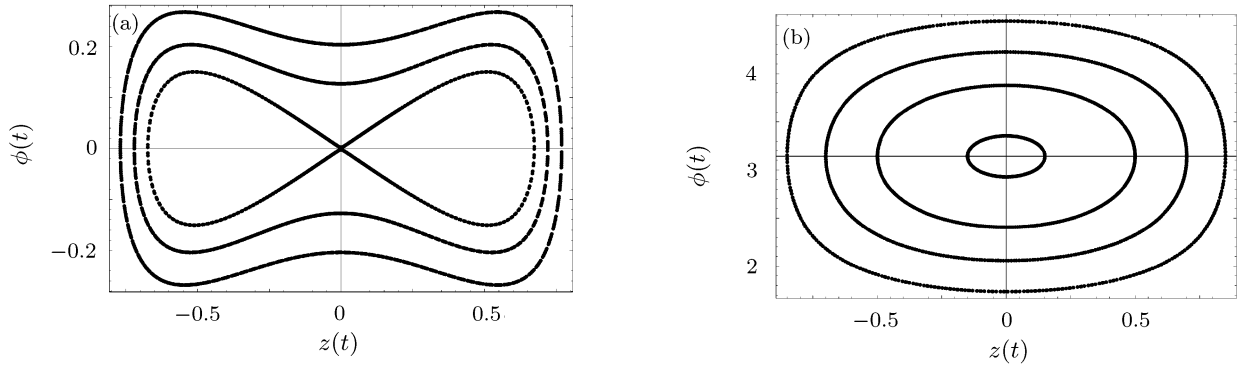


Fig.1. Phase portraits of z vs ϕ for $\Delta E = 0$, $\Lambda = -2.5$ and different initial conditions. (a) Shows that $[z = 0, \phi = 0]$ is a saddle point and (b) indicates that $[z = 0, \phi = \pi]$ is a centre.

3. Chaotic population oscillations under perturbation

Given Eqs.(9) and (10), the Hamiltonian of the system can be expressed as

$$H = \frac{\Lambda}{2}z^2 + \Delta E z - 2\sqrt{1-z^2}\cos\phi. \qquad (11)$$

From Eqs.(9)–(11) we can easily obtain the second-order derivative of $z(t)$ with respect to time as

$$\ddot{z} = -4z - \Big(+\frac{\Lambda}{2}z^2 + \Delta E z - H\Big)(\Delta E + \Lambda z) - \eta\dot{z}(t). \qquad (12)$$

We consider the case with the parameters Λ and ΔE bearing the following forms:

$$\Lambda = \Lambda_0 + \Lambda_1\sin(\omega t), \quad \Delta E = \Delta E_0 + \Delta E_1\sin(\omega t) \quad (13)$$

with $|\ \Lambda_0\ | \gg |\ \Lambda_1\ | \sim |\ \Delta E_{0,1}\ |$. Here Λ_0 and ΔE_0 are the amplitudes of the dc components; Λ_1 and ΔE_1 are the amplitudes of the ac components. Applying Eq.(13) to Eq. (11) and performing the time derivative of $H(z, \phi, t)$, we reach

$$\begin{aligned}\dot{H}(t) &= \frac{\partial H}{\partial z}\dot{z} + \frac{\partial H}{\partial \phi}\dot{\phi} + \frac{\partial H}{\partial t} \\ &= \frac{\partial H}{\partial t} = \frac{z^2}{2}\frac{\partial \Lambda}{\partial t} + \frac{\partial \Delta E}{\partial t}z \\ &= \Big(\frac{z^2\Lambda_1\omega}{2} + z\omega\Delta E_1\Big)\cos(\omega t)\,. \end{aligned} \qquad (14)$$

Integration of Eq.(14) over the dimensionless time t results in

$$\begin{aligned} &H(t) = H_0 + H_1(t), \\ &H_1(t) = \int\Big(\frac{z^2\Lambda_1\omega}{2} + z\omega\Delta E_1\Big)\cos(\omega t)\mathrm{d}t, \end{aligned} \qquad (15)$$

where H_0 is a constant and $H_1(t)$ is a first-order small term proportional to ΔE.[13] Inserting Eqs.(13) and

(15) into Eq.(12), we obtain

$$\ddot{z} - (\Lambda_0 H_0 - 4)z + \frac{\Lambda_0^2}{2}z^3 = \Lambda_0 H_1 z + \Lambda_1 H z \sin(\omega t) - \Big(\Lambda_0 \Lambda_1 \sin(\omega t) + \frac{1}{2}\Lambda_1^2 \sin^2(\omega t)\Big) z^3 - \frac{3\Delta E \Lambda}{2} z^2 - \Delta E^2 z + H \Delta E - \eta \dot{z}. \quad (16)$$

When the right-hand side of Eq.(16) equals zero, the system is clearly integrable and possesses a separatrix trajectory, which is an essential demand for the application of the direct perturbation and Melnikov function methods to study the chaotic dynamics of the perturbed system.[13,16,26–29] The dynamical behaviours close to the separatrix is extremely sensitive to the initial conditions and the values of the system parameters, which is one of the leading features of strange chaotic attractors. As has been known, the Melnikov-function method is an effective tool of finding the regions of chaotic dynamics in perturbed systems.[15,36]

In order to use the direct perturbation and Melnikov-function methods to investigate the chaotic population oscillations, we expand the general solution of Eq.(16) to the first order

$$z = z_0 + z_1, \quad \text{for} \mid z_0 \mid \gg \mid z_1 \mid . \quad (17)$$

Substituting Eq.(17) into Eq.(16), we have the following equations:

$$\ddot{z}_0 - (H_0 \Lambda_0 - 4) z_0 + \frac{1}{2}\Lambda_0^2 z_0^3 = 0, \quad (18)$$

$$\ddot{z}_1 - (H_0 \Lambda_0 - 4) z_1 + \frac{3}{2}\Lambda_0^2 z_0^2 z_1 = \varepsilon_1, \quad (19)$$

$$\varepsilon_1 = \Lambda_0 H_1 z_0 - \frac{3}{2}\Lambda_0 \Delta E z_0^2 + H_0 \Delta E + H_0 \Lambda_1 z_0 \sin(\omega t) - \Lambda_0 \Lambda_1 z_0^3 \sin(\omega t) - \eta \dot{z}_0. \quad (20)$$

Here we have assumed

$$\mid z_1 \mid \sim \mid \Lambda_1 \mid \sim \mid \Delta E_{0,1} \mid \sim \mid \eta \mid \sim \mid H_1 \mid . \quad (21)$$

According to the equilibrium condition $\dot{z}_0 = \ddot{z}_0 = 0$, we can easily obtain three equilibrium solutions of Eq.(18): $z_0 = 0, \pm\sqrt{2(H_{0\Lambda_0} - 4)}/\Lambda_0$. In addition to the equilibrium solutions, Eq.(18) possesses the well-known periodical solution for $(H_0\Lambda_0 - 4) < 0$ and homoclinic solution for $(H_0\Lambda_0 - 4) > 0$. In the present work, we consider only the homoclinic solution usually associated with chaos,

$$z_0 = \frac{2}{\Lambda_0}\sqrt{H_0\Lambda_0 - 4}\,\mathrm{sech}\xi, \quad (22)$$

with $\xi = \sqrt{H_0\Lambda_0 - 4}(t - t_0)$ and t_0 being the initial time. This is a homoclinic solution associated with chaos. Through Eq.(22) we can obtain two linear independent solutions of Eq.(19) when $\varepsilon_1 = 0$

$$f_1 = \frac{\mathrm{d}z_0}{\mathrm{d}t} = -\frac{2}{\Lambda_0}(H_0\Lambda_0 - 4)\,\mathrm{sech}\xi\,\tanh\xi, \quad (23)$$

$$f_2 = f_1 \int (f_1)^{-2}\mathrm{d}t = \frac{\Lambda_0}{4\sqrt{(H_0\Lambda_0 - 4)^3}}\,\mathrm{sech}\xi\,(2 - 3\xi\tanh\xi - \sinh^2\xi). \quad (24)$$

It is known that (z_0, f_1) is just the separatrix solution. In our perturbation analysis and using Melnikov function method to study the Smale-horseshoe chaos, we consider the oscillation of the population imbalance close to the separatrix solution. Evidently, f_2 is unbounded and will exponentially increase with the growth of t due to its inclusion of hyperbolic sine function. Using Eqs.(23) and (24) and through variation of constants, we construct the general solution of Eq.(19)[13,16,26–29]

$$z_1 = f_2 \int_{C_1}^{t} f_1 \varepsilon_1 \mathrm{d}t - f_1 \int_{C_2}^{t} f_2 \varepsilon_1 \mathrm{d}t. \quad (25)$$

Here C_1 and C_2 are two arbitrary constants determined by the initial conditions. Applying Eqs.(20), (23) and (24) to Eq.(25) and carefully calculating the limits for $t \to \infty$, we find

$$\lim_{t\to\pm\infty} z_1 \to \pm\infty, \quad (26)$$

due to the inclusion of the unbounded function f_2 in Eq.(25). Equation (26) indicates that the general solution (25) is Lyapunov unstable.[38] Fortunately, if the conditions

$$G_\pm = \lim_{t\to\pm\infty} \int_{C_1}^{t} f_1 \varepsilon_1 \mathrm{d}t = 0 \quad (27)$$

are satisfied, this kind of instability can be controlled, namely, solutions (25) can be Lyapunov stable.[38] The Refs.[13, 16, 26–29] have proved that $G_+ - G_- = 0$ can eliminate the constant C_1 and lead to the well-known Melnikov function

$$\Delta M(t_0) = \int_{-\infty}^{+\infty} f_1 \varepsilon_1 \mathrm{d}t = 0, \quad (28)$$

which predicts the onset of Smale-horseshoe chaos in the oscillations of the population imbalance. Inserting Eqs.(20) and (22) into Eq.(28) and performing the integration in it, we find the Melnikov chaotic criterion

$$\Delta M(t_0) = \Delta E_1 \pi\omega\Big[\frac{D^2 + \omega^2}{\Lambda_0} - H_0\Big] \times \cos(\omega t_0)\mathrm{sech}\Big(\frac{\omega\pi}{2D}\Big)$$

$$+\frac{\Lambda_1\pi\omega^2}{\Lambda_0}\Big[\frac{4\mathrm{D}^2+\omega^2}{3\Lambda_0}-H_0\Big]\cos(\omega t_0)$$
$$\times\,\mathrm{csch}\Big(\frac{\omega\pi}{2D}\Big)-\frac{4\eta D^3}{3\Lambda_0}=0 \qquad (29)$$

with $D=\sqrt{H_0\Lambda_0-4}$. Melnikov function is proportional to the distance between the stable and unstable manifolds in the Poincaré section at t_0. If the Melnikov function has simple zeros, the transverse intersection of the stable and unstable manifolds will occur. This is an indication of the existence of chaotic oscillations of the population imbalance in the system.

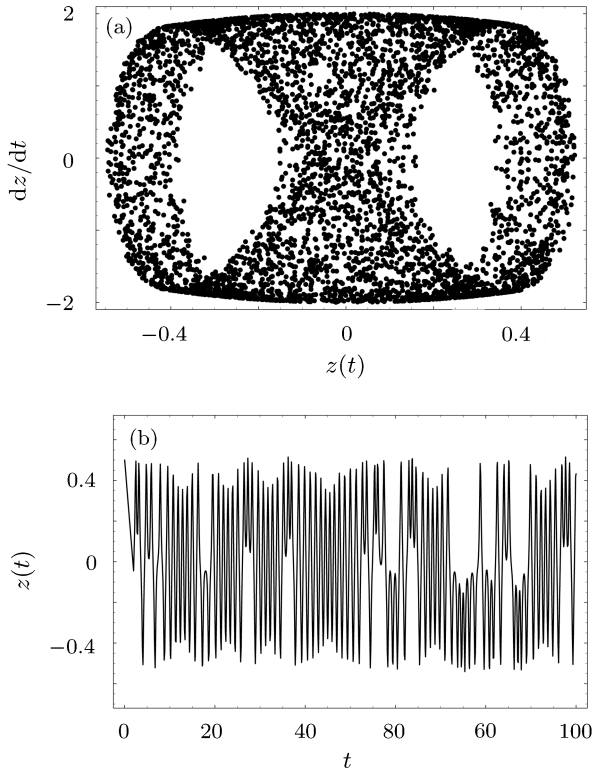


Fig.2. The phase portrait in $(z,\dot{z})$ plane and time-evolution of z with $\Delta E_0=0.5$, $\Delta E_1=0.5$, $\Lambda_0=28$, $\Lambda_1=0.7$, $\eta=0$, $\omega=5$, $z(0)=0.5$, and $\phi(0)=0$.

In order to exhibit the chaos in the perturbed system, with a set of fixed system parameters and initial conditions we plot the phase portrait in the $(z,\dot{z})$ plane and the corresponding time-evolution of $z(t)$ in Figs.2(a) and 2(b), respectively. From Fig.2(a) we can find that the phase orbit evolves in a finite region and exhibits confusion, which is the chaotic feature. Figure 2(b) demonstrates the typical chaotic oscillation of the population imbalance. The Fourier power spectrum of z is presented in Fig.3 with the same parameters as those in Fig.2. From Fig.3 we see a continuous power spectrum with a broadband feature. To the best of our knowledge, such a power spectrum shows the existence of chaos.

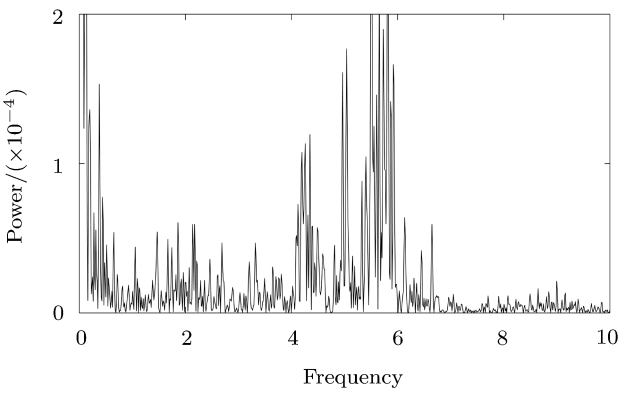


Fig.3. The Fourier power spectrum of the population imbalance $z(t)$ with the same parameters as those in Fig.2.

4. Unperturbed numerical simulations

When the system does not satisfy the perturbation conditions, e.g. the population oscillations are not close to the separatrix solution, the trap potential is large, $\Lambda_0=0$, or Λ_0 and Λ_1 are of the same order, the perturbation and Melnikov function methods will be invalid. Hence, in this section we will perform only numerical simulations of the population oscillations to investigate the dynamical behaviours of the system.

Whether the double-well trap is symmetric or asymmetric in the nondissipative regime ($\eta=0$), we can observe period doubling with the increase of the value of parameter Λ_1. It has been known that period doubling is an important path leading to chaos in some nonlinear systems. To illustrate period doubling in our system, we consider the case of a symmetric double-well potential ($\Delta E=0$) in the nondissipative regime ($\eta=0$). According to Eqs.(9) and (10), by fixing $\Lambda_0=0$, $\omega=1.5$, $z(0)=0.5$, and $\phi(0)=0$, we plot Fig.4 with the increasing Λ_1. The left column of Fig.4 is the phase portraits in the (z, $\dot{z}$) plane formed from $t=0$ to $t=40$; the right column is the corresponding time evolutions of z. When $\Lambda_1=0.02$, there is only one orbit in the (z, $\dot{z}$) plane, which indicates that the oscillation is singly periodic. When the value of Λ_1 increases to 0.5, the period doubling is clearly observed in the phase space. If Λ_1 further increases to 0.72, a period-4 attractor appears. And while $\Lambda_1=3.1$, chaotic oscillation occurs. From the right column of Fig.4 we can see that the corresponding time evolutions of the population imbalance z also

illustrate the process from period doubling to chaos. The chaotic oscillation of the population imbalance indicates that the atomic tunnelling between the two BECs is chaotic.

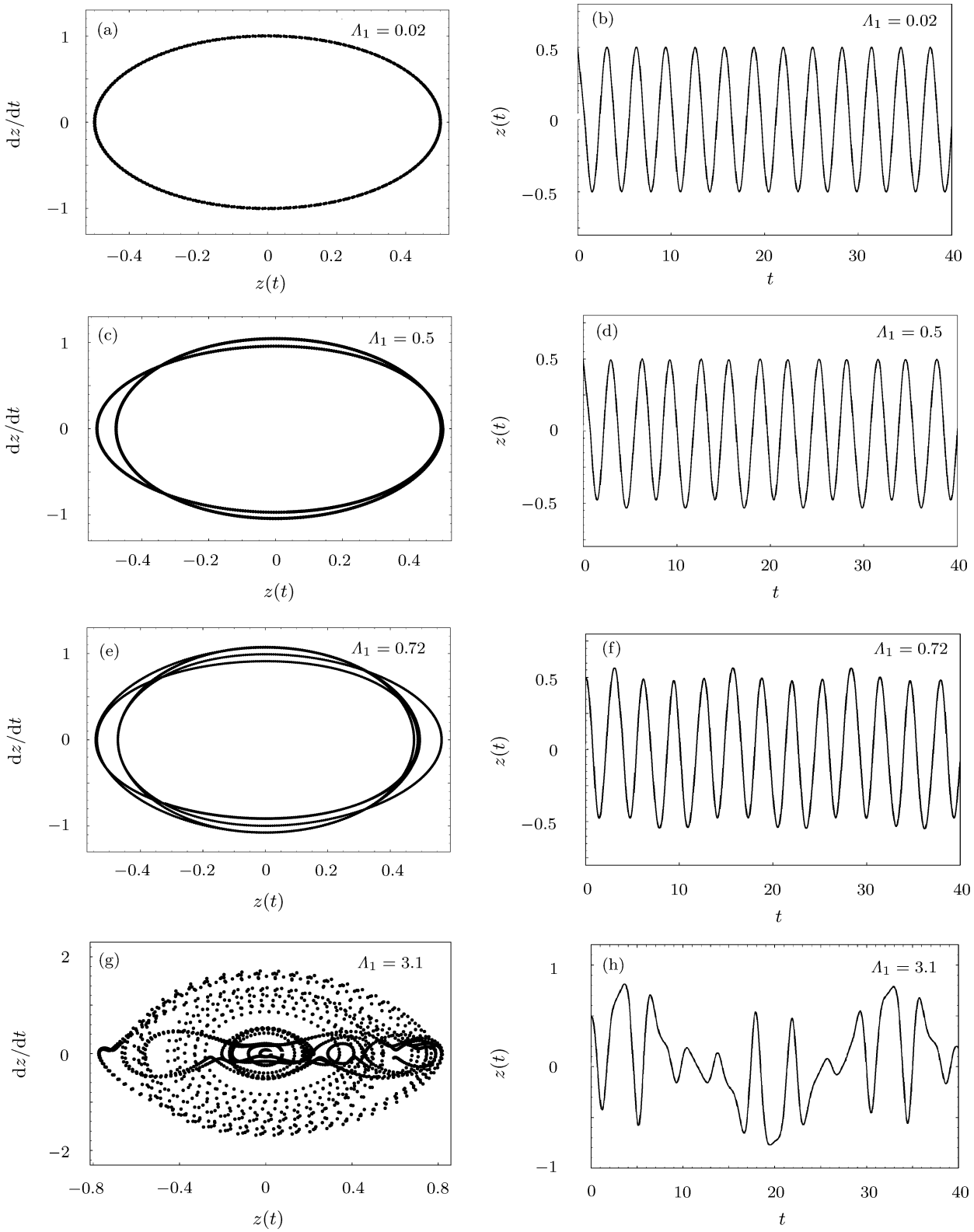


Fig.4. The left column is the phase portrait in the $(z,\ \dot{z})$ plane formed from $t = 0$ to $t = 40$; the right column is the corresponding time evolution of z.

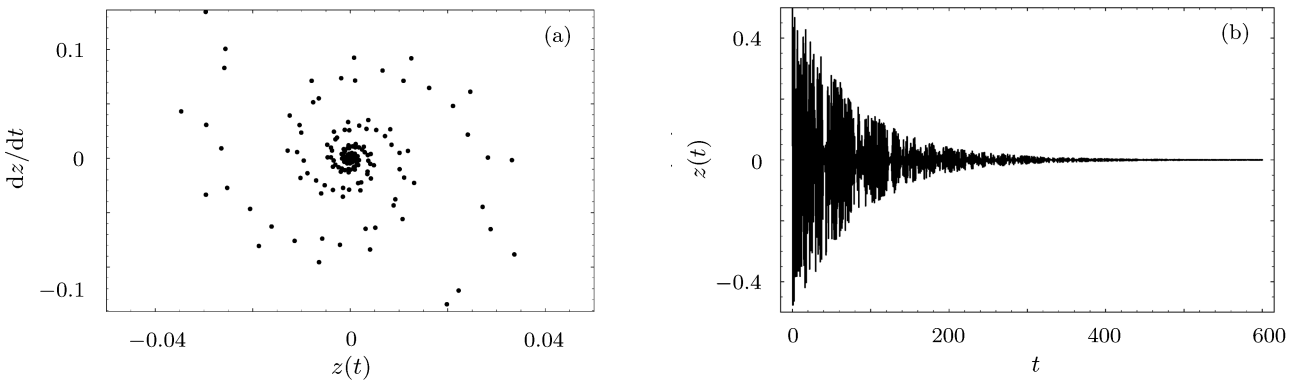


Fig.5. The left is the phase portrait in the $(z,\ \dot{z})$ plain formed from $t = 0$ to $t = 600$; the right is the corresponding time evolution of z.

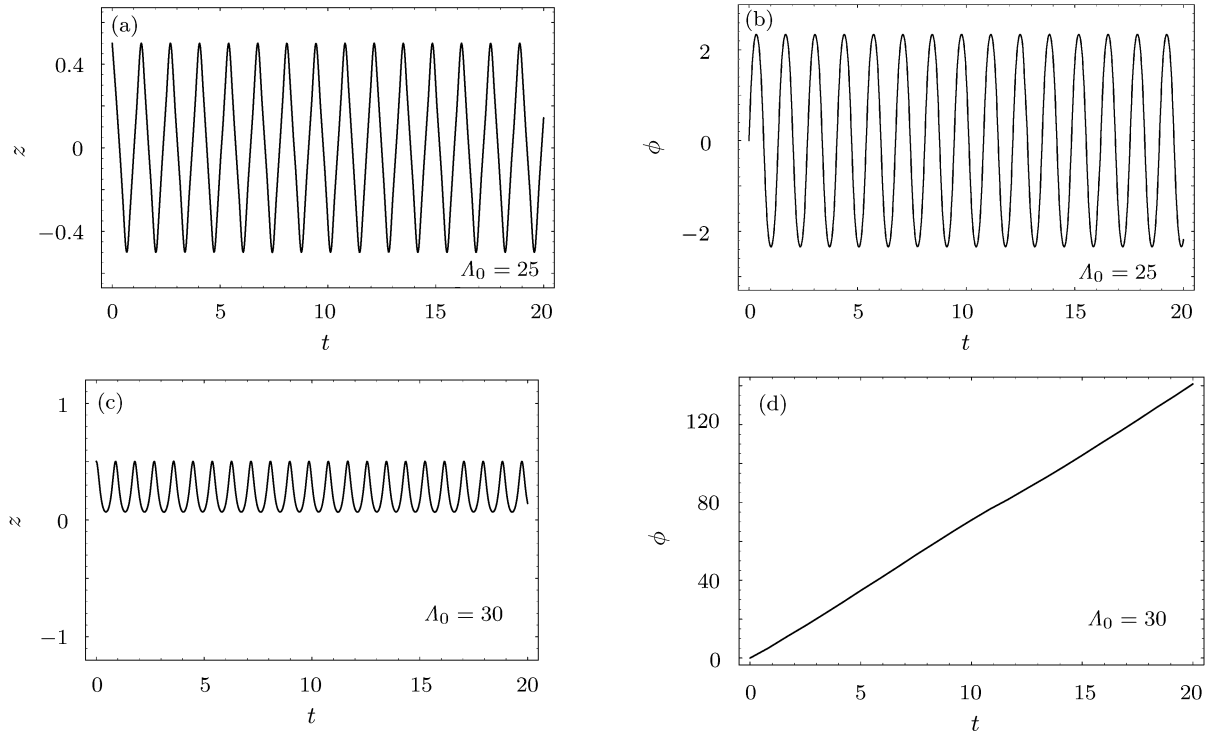


Fig.6. Time evolutions of z and ϕ. The first row with $\Lambda_0 = 25$ shows that both the population imbalance and the relative phase oscillate periodically with a finite amplitude; the second row with $\Lambda_0 = 30$ indicates that the population imbalance oscillates with only a small amplitude and the relative phase increases monotonically, which correspond to the running-phase macroscopic quantum self-trapping.

To the best of our knowledge, the phase space volume always tends to decrease due to the damping force in a period of transient time; and when the damping is strong enough, the phase space volume will decrease to zero, which indicates that the oscillation of z arrives at an equilibrium state with zero population imbalance. This can be seen in Fig.5 for the symmetric potential case ($\Delta E = 0$) with $\Lambda_0 = 8$, $\Lambda_1 = 2$, $\omega = 1$, $\eta = 0.025$, $z(0) = 0.5$, and $\phi(0) = 0$. The left of Fig.5 is the phase portrait in the $(z,\ \dot{z})$ plane formed from $t = 0$ to $t = 600$; the right is the corresponding time evolution of z showing that the oscillation reaches an equilibrium state with zero population imbalance. Now, we consider the influence of Λ_0 on the oscillations of the population imbalance. We plot Fig.6 with $\Delta E = 0$, $\Lambda_1 = 0.5$, $\eta = 0$, $\omega = 1.5$, $z(0) = 0.5$, $\phi(0) = 0$, and

different values of Λ_0. From the first row of Fig.6 one can see that when $\Lambda_0 = 25$ the population imbalance and the relative phase oscillate periodically with finite amplitudes; however, when the value of Λ_0 increases to 30, z exhibits only small amplitude oscillation that never crosses $z = 0$, i.e. $\langle z \rangle \neq 0$, and the corresponding relative phase is unbound and winds up over time. The small amplitude oscillation and monotonically increasing relative phase are two typical characteristics of macroscopic quantum self-trapping related to the running phase modes. This is in agreement with the newly observed experimental results reported by Albiez *et al.*[20]

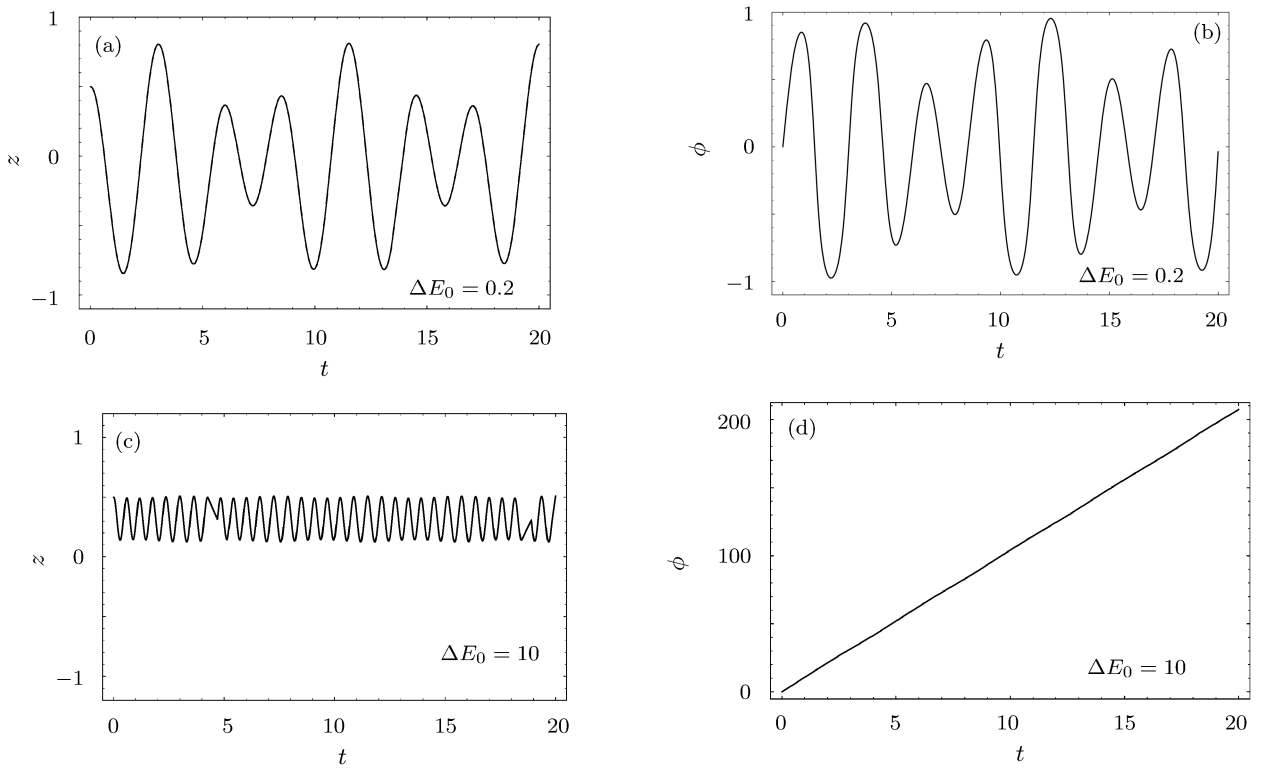


Fig.7. Time evolutions of z and ϕ. The first row with $\Delta E_0 = 0.2$ shows that both the population imbalance and the relative phase oscillate with a finite amplitude; the second row with $\Delta E_0 = 10$ corresponds to the running-phase macroscopic quantum self-trapping.

When the double-well potential is an asymmetric one ($\Delta E \neq 0$), one can see the influence of the asymmetric potential on the oscillations of the population imbalance clearly. In this case the increase in the value of ΔE_0 can also result in MQST. After assuming $\Delta E_1 = 0.5$, $\Lambda_0 = 0.5$, $\Lambda_1 = 0.1$, $\eta = 0$, $\omega = 1.5$, $z(0) = 0.5$, $\phi(0) = 0$, and different values of ΔE_0, we plot Fig.7. From Fig.7 one can observe that when $\Delta E_0 = 0.2$ both the population imbalance and the relative phase oscillate with finite amplitudes; but when ΔE_0 increases to 10 the running-phase macroscopic quantum self-trapping appears. It is also found that in the presence of a weak asymmetric trap potential, there exist parametric resonances in the oscillations of the population imbalance as shown in Fig.8 with $\Delta E_0 = 0.02$, $\Delta E_1 = 0.02$, $\Lambda_0 = 0$, $\eta = 0$, $\omega = 4$, and $\phi(0) = 0$. The first row of Fig.8 is for $\Lambda_1 = 0.4$ and $z(0) = 0.81$; the second row is for $\Lambda_1 = 0.092$ and $z(0) = 0.2$. Parametric resonance is a kind of more complicated resonant behaviour, where a relevant parameter of the system is modulated to achieve resonance.[39] In Bose–Einstein condensates systematical studies on parametric resonance have been extensively performed.[39–43]

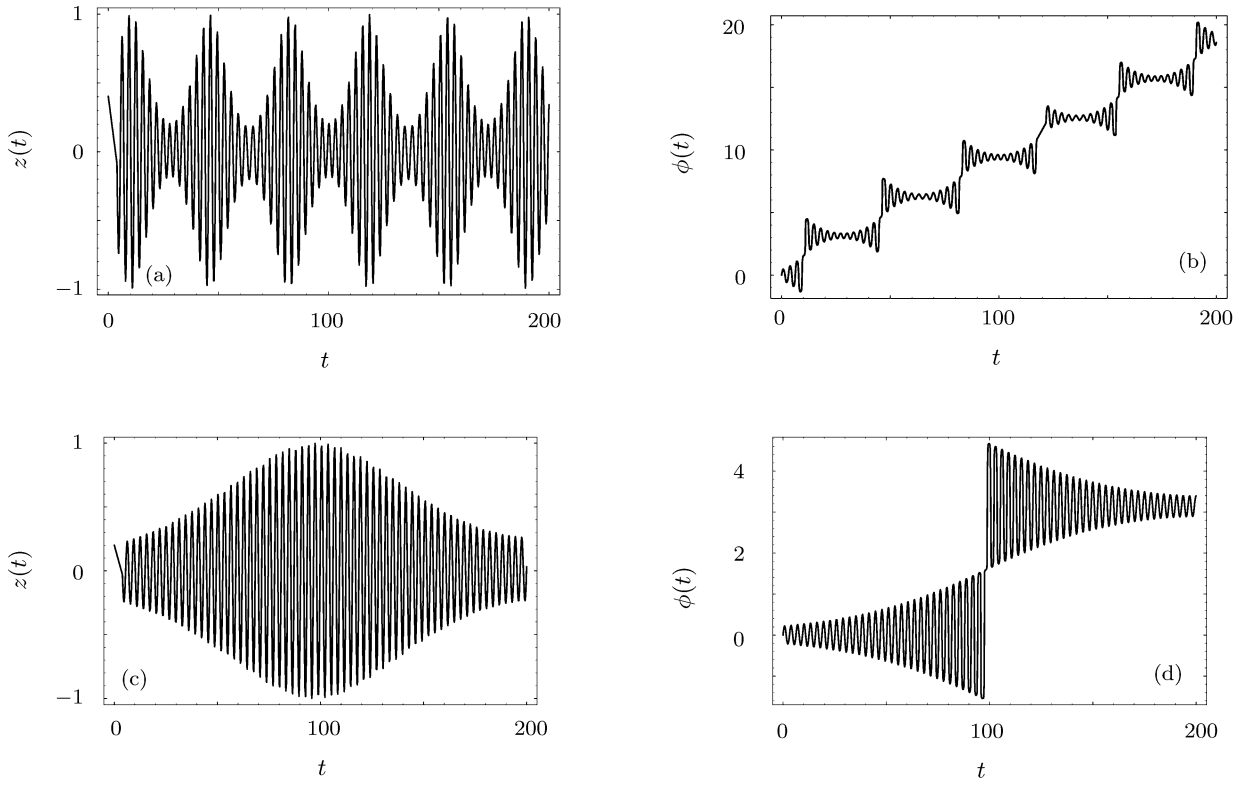


Fig.8. When the asymmetric trap potential is weak, the parametric resonance appears. The parameters are set as $\Delta E_0 = 0.02$, $\Delta E_1 = 0.02$, $\Lambda_0 = 0$, $\eta = 0$, $\omega = 4$, and $\phi(0) = 0$. The first row is for $\Lambda_1 = 0.4$ and $z(0) = 0.81$; the second row is for $\Lambda_1 = 0.092$ and $z(0) = 0.2$.

5. Discussion and conclusion

In summary, we have studied the atomic population oscillations between two coupled Bose–Einstein condensates with time-dependent nonlinear interaction in a double-well potential. In experiments the position of the laser sheet and the intensity and detuning of the laser are modifiable. Consequently, the trap asymmetry is changeable. Meanwhile, the magnetic field resonantly coupled to the atoms is adjustable. So one can reach the system parameters needed to satisfy experimental conditions. For example, the values of ΔE_1, Λ_0, Λ_1, ω, and D can be successfully regulated to satisfy Melnikov function (29) through adjusting the configuration of the double-well trap and the magnetic field.

With the linear stability theorem we first analyse the stabilities of the steady-state solutions. And then in the perturbative regime, we theoretically obtain a general solution of the perturbed equation. It is found that the boundedness condition of the general solution contains Melnikov chaotic criterion applied to predicting the onset of chaos in perturbed systems. While the system is out of the perturbative regime, we numerically find that the nonlinear interatomic interaction has a crucial influence on the oscillation of the population imbalance while stepping into chaos via period doubling. This shows that changing the nonlinear interatomic interaction through the Feshbach resonances[23−25] can effectively suppress the chaotic oscillations of the population imbalance. The running-phase macroscopic quantum self-trapping and parametric resonances are also numerically investigated.

References

[1] Anderson M H, Ensher J R, Matthews M R, Wieman C E and Cornell E A 1995 *Science* **269** 198
[2] Bardley C C, Sackett C A, Tollett J J and Hulet R G 1995 *Phys. Rev. Lett.* **75** 1687
[3] Davis K B, Mewes M O, Andrews M R, Druten N J, Durfee D S, Kurn D M and Ketterle W 1995 *Phys. Rev. Lett.* **75** 3969
[4] Xie B H and Jing H 2002 *Chin. Phys.* **11** 115

[5] Hu Z F, Du C G and Li S Q 2003 *Chin. Phys.* **12** 0708
[6] Zhang G F, Yin W, Liang J Q and Yan Q W 2004 *Chin. Phys.* **13** 988
[7] Huang G X 2004 *Chin. Phys.* **13** 1866
[8] Wei W 2005 *Chin. Phys.* **14** 2407
[9] Wang G F, Fu L B, Zhao H and Liu J 2005 *Acta Phys. Sin.* **54** 5003 (in Chinese)
[10] Xiao Y F, Wang D L, Wang F J and Yan X H 2006 *Acta Phys. Sin.* **55** 0547 (in Chinese)
[11] Smerzi A, Fantoni S, Giovanazzi S and Shenoy S R 1997 *Phys. Rev. Lett.* **79** 4950
[12] Raghavan S, Smerzi A, Fantoni S and Shenoy S R 1999 *Phys. Rev.* A **59** 620
[13] Hai W, Lee C, Chong G and Shi L 2002 *Phys. Rev.* E **66** 026202
[14] Ruostekoski J and Walls D F 1998 *Phys. Rev. Lett.* **58** R50
[15] Abdullaev F K and Kraenkel R A 2000 *Phys. Rev.* A **62** 023613
[16] Lee C, Hai W, Shi L, Zhu X and Gao K 2001 *Phys. Rev.* A **64** 053604
[17] Gardiner S A, Jaksch D, Dum R, Cirac J I and Zoller P 2000 *Phys. Rev.* A **62** 023612
[18] Weiss C and Jinasundera T 2005 *Phys. Rev.* A **72** 053626
[19] Abdullaev F K 2001 *Phys. Rev.* E **63** 056704
[20] Albiez M, Rudolf G, Jonas F, Stefan H, Matteo C and Markus K O 2005 *Phys. Rev. Lett.* **95** 010402
[21] Ou B, Zhao X, Liu J and Chen S 2001 *Phys. Lett.* A **291** 17
[22] Liu J, Wu B and Niu Q 2003 *Phys. Rev. Lett.* **90** 170404
[23] Cornish S L, Claussen N R, Roberts J L, Cornell E A and Wieman C E 2000 *Phys. Rev. Lett.* **85** 1795
[24] Kagan Y, Surkov E L and Shlyapnikov G V 1997 *Phys. Rev. Lett.* **79** 2604
[25] Abdullaev F K, Caputo J G, Kraenkel R A and Malomed B A 2003 *Phys. Rev.* A **67** 013605
[26] Xie Q, Hai W and Chong G 2003 *Chaos* **13** 801
[27] Chong G, Hai W and Xie Q 2004 *Chaos* **14** 217
[28] Chong G, Hai W and Xie Q 2004 *Phys. Rev.* E **70** 036213
[29] Chong G, Hai W and Xie Q 2005 *Phys. Rev.* E **71** 016202
[30] Li Y and Hai W 2005 *J. Phys.* A **38** 4105
[31] Luo X and Hai W 2005 *Chaos* **15** 033702
[32] Xia B, Hai W and Chong G 2006 *Phys. Lett.* A **351** 136
[33] Fang J, Hai W, Chong G and Xie Q 2005 *Physica* A **349** 133
[34] Lee C, Hai W, Shi L and Gao K 2004 *Phys. Rev.* A **69** 033611
[35] Sakellari E, Proukakis N P, Leadbeater M and Adams C S 2004 *New J. Phys.* **6** 42
[36] Williams J, Walser R, Cooper J, Cornell E and Holland M 1999 *Phys. Rev.* A **59** R31
[37] Orzel C, Tuchman A K, Fenselau M L, Yasuda M and Kasevich M A 2001 *Science* **291** 2386
[38] Hai W, Duan Y, Zhu X, Luo X and Shi L 1998 *J. Phys.* A **31** 2991
[39] Garcia-Ripoll J J and Pérez-Garcia V M 1999 *Phys. Rev. Lett.* **83** 1715
[40] Castin Y and Dum R 1997 *Phys. Rev. Lett.* **79** 3553
[41] Kagan Y and Maksimov L A 2001 *Phys. Rev.* A **64** 053610
[42] Staliunas K, Garcia S and Valcárcel G J 2002 *Phys. Rev. Lett.* **89** 210406
[43] Tozzo C, Krämer M and Dalfovo F 2005 *Phys. Rev.* A **72** 023613